NON - RESONANCE CONTRIBUTION TO GDH SUM RULE

N.BIANCHI and E.THOMAS
INFN - Laboratori Nazionali di Frascati, Via E. Fermi 40,
00044 Frascati, ITALY
E-mail: nicola.bianchi@lnf.infn.it

A parameterisation of the virtual photon absorption cross section difference $\left[\sigma_{1/2} - \sigma_{3/2}\right]$ for the proton and neutron is presented. The Regge inspired parameterisation is obtained from global fits to the cross section data derived from the spin asymmetries measured in deep inelastic scattering of longitudinally polarised leptons from polarised ^{1}H, ^{3}He and ^{2}H targets in the range 0.3 GeV^2 $< Q^2 <$ 70 GeV^2 and 4 GeV^2 $< W^2 <$ 300 GeV^2. An accurate description of the data is provided and a reliable prediction for the photo-production through a smooth Q^2-transition is given. The parameterisation is used to evaluate the contribution above the resonance region to the Gerasimov-Drell-Hearn sum rule for real and virtual photons. The main result is the large high-energy and multi-hadron contribution to the GDH sum rule, particularly in the isovector channel. Taking into account this large contribution, together with previous estimates of single-pion and resonance contributions, the GDH sum rule seems to be fulfilled.

1 Introduction

One of the most important topic of the modern hadronic physics is the study of the polarisation variables. In particular, an interesting and almost unknown quantity is the difference of the cross sections $\Delta\sigma = \left[\sigma_{1/2} - \sigma_{3/2}\right]$ in which $\sigma_{1/2}$ and $\sigma_{3/2}$ are the photon-nucleon absorption cross sections of total helicity 1/2 and 3/2, respectively. A fundamental sum rule for this quantity has been derived by Gerasimov, Drell and Hearn [1] (GDH). It relates the anomalous contribution κ to the magnetic moment of the nucleon ($\kappa_{\rm p}$=1.79, $\kappa_{\rm n}$=−1.91) with the total absorption cross sections for circularly polarised real photons on polarised nucleons. It is given by:

$$I = \int_{\nu_0}^{\infty} \Delta\sigma(\nu)\frac{d\nu}{\nu} = -\frac{2\pi^2\alpha}{m^2}\kappa^2, \qquad (1)$$

where ν is the photon energy, ν_0 is the pion photoproduction threshold and m is the nucleon mass. The theoretical predictions for the integral are –204 μb, –233 μb and +29 μb for the proton, neutron and proton-neutron difference (p-n), respectively. Experimentally this sum rule has never been tested directly because of the lack of suitable polarised targets and real photon beams. Several experiments [2] are now running or planned at different facilities to measure the spin-dependent photo-production cross section in the nucleon resonance region

and up to about 3 GeV. Multipole analysis of single pion photo-production amplitudes and estimates of the double pion contribution from the nucleon resonance decays provided an indication of the low energy contribution to the sum rule, which is expected to be the dominant one. These estimates were qualitatively consistent among each others providing results ranging between –289 and –257 μb, –189 and –169 μb, –130 and –68 μb for the proton, neutron and proton-neutron difference respectively [3,4]. All these findings strongly disagree with the GDH expectations and suggested a possible violation of the sum rule. In particular the multipole analysis of the isovector channel (i.e. the proton-neutron difference) provides an opposite sign of the sum rule expectation.

Unfortunately up to now, no estimate is available for the spin-dependent photo-production cross section at high energies which should be dominated by inelastic non-resonance channels in which many hadrons are produced. Here we present the first evaluation of this cross section and the first evaluation of its contribution to the GDH sum rule. The latter was found to be large and to be the dominant contribution for the isovector sum rule. The spin-dependent photo-production cross section has been evaluated from a smooth extrapolation of the spin-dependent electro-production cross section measured in several Deep Inelastic Scattering (DIS) experiments. More details on this work can be found in Ref. [5]. A Regge inspired parameterisation was used.

2 Regge phenomenology

The Regge theory provided a good description of the high-energy behaviour of the cross sections for a large number of processes [6]. In this framework the cross section behaviours are given by $\sigma \sim s^{\alpha^0-1}$ where s is the center of mass square energy and α^0 is the intercept of the leading Regge trajectory for the given process. The intercept $\alpha^0 = J - \alpha' m_t^2$ is determined by the spin J and mass m_t of the exchanged particle and by the trajectory slope $\alpha' \simeq$ 0.8-0.9 GeV^{-2}. In the case of the absorption of circularly polarised photons on polarised nucleon it is useful to consider the isovector and the isoscalar terms of the interaction [7]. The isovector contribution to $\Delta\sigma$ is described by the $a_1(1260)$ meson trajectory : $\Delta\sigma_V \sim s^{\alpha^0_{a1}-1}$. The axial vector meson a_1 is still now an elusive prey in most of experiments due to its large width and the presence of strong background. Experiments of the last twenty years provided contradictory measurements of the a_1 meson mass and width over the wide ranges 1.05-1.28 GeV and 0.24-0.61 GeV, respectively [8]. The expected value of the a_1 meson intercept is about -0.3, but due to the uncertainties in the knowledge of the mass and of the trajectory slope, a possible range between 0

and -0.5 is generally considered. The isoscalar contribution to $\Delta\sigma$ is described by the $f_1(1285)$ meson trajectory $\Delta\sigma_I \sim s^{\alpha^0_{f_1}-1}$. Being the f_1 meson mass well known, its intercept is expected to be about -0.4 ± 0.1. In addition it has been shown that the exchange of two non-perturbative gluons can provide an isoscalar contribution $\Delta\sigma_I \sim (1/s)ln(s/\mu^2)$ where the mass parameter μ has the typical hadronic scale $\mu \sim 1$ GeV [9]. In this work we consider the above described contributions for the case of photo-absorption of circularly polarised virtual photon on polarised nucleon where the centre of mass square energy is given by $W^2 = m^2 + 2m\nu - Q^2$.

3 Data analysis and fitting procedure

We have analysed the data from deep inelastic scattering of longitudinally polarised leptons off polarised ^{1}H, ^{2}H and ^{3}He targets which provided measurements of the photo-absorption asymmetry A_1 for the proton, deuteron and neutron respectively. The measurements were performed by six experiments at CERN (EMC [10], SMC [11]), SLAC (E142 [12], E143 [13], E154 [14]) and DESY (HERMES [15]). For each experiment we considered the data set with the most detailed Q^2 and x binnings. A total of 511 independent data points was included in the analysis: specifically 238 proton data, 81 neutron data and 192 deuteron data. The kinematic range covered by the data is 0.3 GeV$^2 < Q^2 <$ 70 GeV^2 and 4 GeV$^2 < W^2 <$ 300 GeV^2 for the proton and deuteron, and 1 GeV$^2 < Q^2 <$ 15 GeV^2 and 4 GeV$^2 < W^2 <$ 70 GeV^2 for the neutron.

The cross section difference $\Delta\sigma$ was derived from the measured virtual photo-absorption asymmetry A_1 and from the unpolarised structure function F_1:

$$\Delta\sigma = 2A_1\sigma_T = \frac{8\pi^2\alpha}{m}\,\frac{A_1F_1}{K}, \qquad (2)$$

where σ_T is the total transverse cross section and $K = \sqrt{\nu^2 + Q^2}$ is the virtual photon flux factor. The structure function $F_1 = F_2(1+\gamma^2)/(2x(1+R))$ was calculated from published parameterisations of the unpolarised structure functions F_2 for the proton, neutron and deuteron and of $R = \sigma_L/\sigma_T$, the ratio of the absorption cross sections for longitudinally and transversely polarised virtual photons.

The $\Delta\sigma$ experimental data were reproduced by a global 3-Dimensional fit over the Q^2 and W^2 variables and the isospin dimension T:

$$\Delta\sigma = \Delta\sigma(T, W^2, Q^2) = \left[2aW^{2(\alpha^0_{a1}-1)}T + fW^{2(\alpha^0_{f_1}-1)} + g\frac{lnW^2}{W^2}\right]F, \qquad (3)$$

where F is the threshold factor

$$F = \left[\frac{W^2 - W_\pi^2}{W^2 - W_\pi^2 + Q^2 + m_r^2} \right]^p , \tag{4}$$

where W_π is the single pion electro-production threshold and $m_r = 1.26$ GeV is a common mass scale of the exchanged particles which is close to the a_1 and f_1 meson masses and to the two gluon exchange hadronic scale. The exponent p is given by

$$p = 1.5 \left(1 + \frac{Q^2}{Q^2 + M^2} \right) , \tag{5}$$

being M a free parameter of the fit. This threshold factor is similar to the ones used in the description of unpolarised cross section σ_T accounting for the behaviour of a cross section corresponding to a virtual particle with $W^2 > Q^2$ [16,17,18].

Because Regge theory gives no indication about the relative weight and Q^2-dependence of the various contributions, the three coefficients in eq. 3 were parametrised with a simple and smooth Q^2-dependence, with two free parameters each :

$$a, f, g = p_1^{a,f,g} + p_2^{a,f,g} t, \tag{6}$$

where

$$t = log \frac{log \frac{Q^2+Q_0^2}{\Lambda^2}}{log \frac{Q_0^2}{\Lambda^2}}. \tag{7}$$

Here Λ and Q_0^2 are the QCD cutoff and scale parameters, respectively. We used $\Lambda = 0.255$ GeV and $Q_0^2 = 0.278$ GeV^2 in agreement with the ALLM parameterisation for the unpolarised total transverse cross section σ_T[17].

The cross section difference for the proton and neutron were defined by eq. 3 with T=+1/2 and T=−1/2, respectively. The cross section difference for the deuteron was defined $\Delta\sigma^d = [\Delta\sigma^p + \Delta\sigma^n]\,(1 - 1.5\omega_D)$ where $\omega_D = 0.05$ is the D-wave probability in the deuteron.

4 Results

We used three slightly different models to reproduce the $\Delta\sigma$ data. Model I is described above. In Model II a smooth Q^2-dependence of a_1-meson intercept was considered. In Model III we considered an additional reggeon trajectory

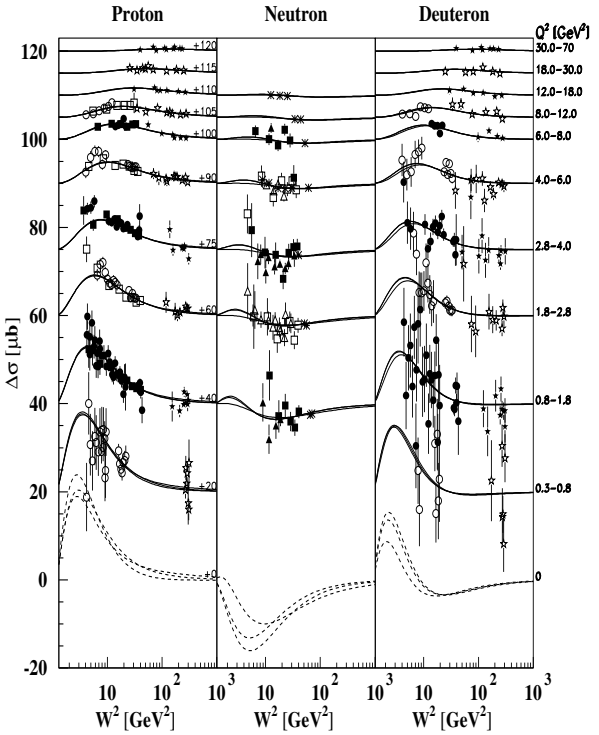

Figure 1: Cross section differences as a function of W^2 for different Q^2-bins (on the right scale). Experimental data are : stars[10,11], triangles[12], circles[13], asterisks[14], and squares[15]. For a better view, a Q^2-increasing constant value (on the right side of the proton panel) has been added to the data which are presented with open and close symbols alternatively. Only data with statistical error lower than 10 μb are shown. The solid curves are the results of the three Models calculated for the average Q^2-values in each Q^2-bin. The dashed curves are the predictions of the three Models for Q^2=0.

$2rW^{2(\alpha_r^0-1)}T$ for the isovector part of the interaction. All the three Models provide a rather good description of the present data. The comparison between the results of the three Models and the experimental data as function of the three variables (T, W^2 and Q^2) is shown in fig. 1. For this purpose the data are presented grouped in Q^2-bins.

In fig. 1 are also shown the results of the three Models for Q^2=0. The expectations for real photons above the resonance region ($W^2 \geq 4$ GeV^2) are: $\Delta\sigma^p$ is clearly positive, $\Delta\sigma^n$ is clearly negative, while $\Delta\sigma^d$ is small and close to 0. As it is seen the low energy part ($W^2 \leq 4$ GeV^2) is more model dependent, being not constrained by the data. The corresponding real photon asymmetries A_1 above the resonance region can be evaluated by dividing $\Delta\sigma$

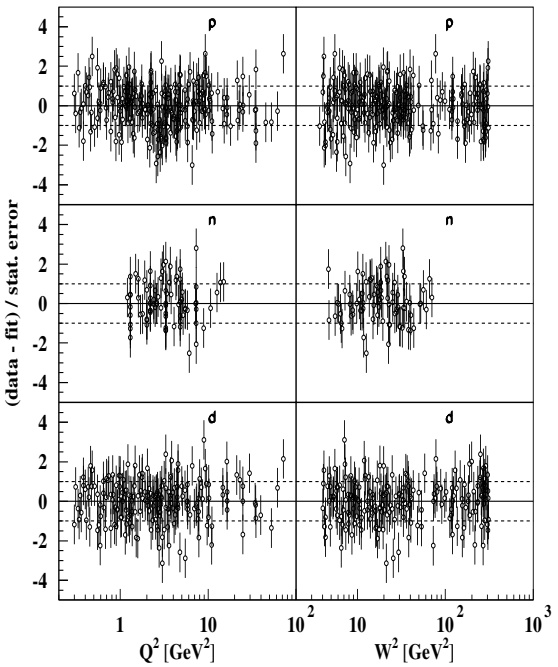

Figure 2: Deviation of the experimental data from the curves of Model II, normalised by the experimental statistical error, as function of Q^2 and of W^2 for the proton, neutron and deuteron.

by $2\sigma_T \sim 240\mu$b. These findings are in qualitative agreement with a recent measurement of the inclusive hadron photoproduction asymmetry [19].

In fig. 2 the point to point difference between the fit and the experimental data is provided. The difference has been normalised by the statistical error of each data point. As it is seen the fit well reproduces all the data over the two orders of magnitude variation of the Q^2 and W^2 variables. The uniform distribution of this difference evidences the good quality of the fit and ensures a reliable extrapolation to $Q^2 = 0$.

5 Contribution to the GDH integral

Our parameterisation has been used for an accurate evaluation of the Q^2-dependence of the high-energy contribution ($W \geq 2$ GeV) to the generalised GDH integral [5]. The estimate is in very good agreement with experimental

Table 1: Evaluation of the GDH integral I_{TOT} for the proton, neutron and proton-neutron difference and comparison with the relevant GDH sum rule expectations. I_{TOT} is computed by the sum of the predicted contributions for single-pion photo-production, double-pion photo-production from the decay of the nucleon resonances N^*, and for the high-energy ($W \geq 2$ GeV) and low-energy ($W < 2$ GeV) multi-hadron ($n_h \geq 2$)photo-production.

	I_p [μb]	I_n [μb]	I_{p-n} [μb]
Resonance and 1π			
$I_{N\pi}$(Drechsel)	-196	-145	-51
$I_{N^* \to N\pi\pi}$(Karliner)	-65	-35	-30
Multi-hadron ($W_{2\pi}$)			
$I_{he}(W \geq 2GeV)$(this work)	$+25 \pm 6$	-36 ± 10	$+61 \pm 12$
$I_{le}(W \leq 2GeV)$(this work)	$+19 \pm 13$	-9 ± 13	$+28 \pm 23$
I_{TOT}	-217 ± 18	-220 ± 22	$+8 \pm 32$
GDH sum rule	-204	-233	$+29$

measurements and in particular with the Bjorken sum rule expectation.

The real photon limit of the high-energy contribution to the GDH integral for the proton, neutron and proton-neutron difference are listed in Table 1. Here we consider the 2-pion threshold $W_{2\pi}$ in eq. 4. The three Model predictions are consistent among each other within $\sim 10\%$. In Table 1 the evaluations of the low-energy parts $I_{le}(0)$ are also presented. The latter results are more model dependent respect to the high-energy contributions and are strongly affected by the choice of the threshold factor F. Moreover $I_{le}(0)$ is less constrained by the experimental data and therefore provides only an approximate estimate of the multi-hadron and non-resonant photo-production contribution at low energy.

The quoted errors for the integrals were derived considering both the contribution of the free parameter errors and the contribution of the fit parameterisation. The latter, which is the dominant one for the real photon extrapolation, has been evaluated from the slightly different predictions of the three models, from varying the fixed parameters of the fit (Q_0^2, Λ^2, m_r^2) within a factor two around the chosen values and from a Q^2-independent choice of the power expression of the threshold function F.

In Table 1 we also reported the contributions from the most recent analysis of single-pion photo-production in both resonant and non-resonant channels [4] and from the decay of the nucleon resonances in two-pions [3]. As it is seen the discrepancies between the sum of these two latter contributions and the

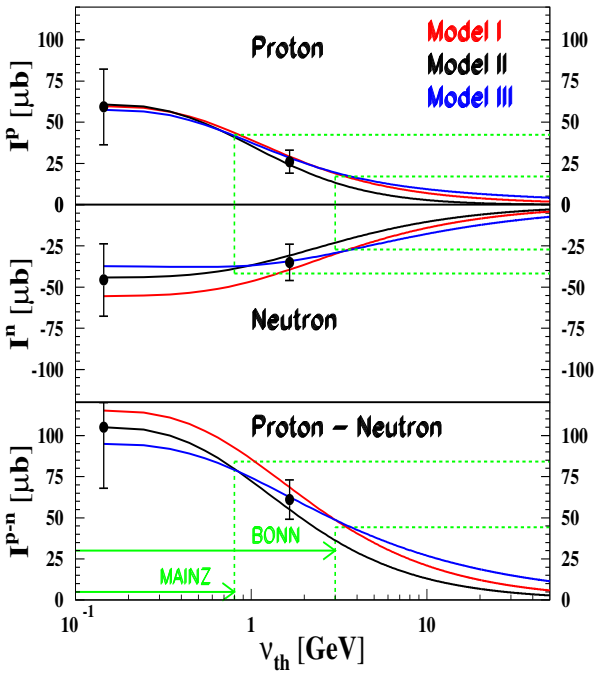

Figure 3: Multi-hadron contribution to the GDH sum rule for the three Models and as function of the lower energy integration limit. Also shown are the ranges of the Mainz and Bonn measurements. The points are the high energy and the total multi-hadron contributions averaged between the three Models.

GDH sum rule expectation is reduced by a factor ≥ 2 if we add our results for the high-energy contributions. Moreover the above discrepancies are almost canceled if we also include our estimates for the low-energy region.

Therefore the evaluation of multi-hadron photoproduction processes accounts for a relevant fraction of the GDH expectations for the proton and the neutron. In addition it represents the largest contribution for the isovector sum rule, in which the resonance contribution is mostly canceled. In fig. 3 the multi-hadron contribution to the GDH sum rule is presented as a function of the lower integration limit for the real photon energy ν_{th}. As it is seen for the isovector sum rule a large contribution ($\sim$ 45 μb) is expected above 3 GeV which is the maximum energy for the measurement planned in Bonn. Therefore to have a full check of the sum rule (for real and quasi-real photons) a measurement which covers few tenths of GeV is needed.

6 Conclusions

We have studied the deep inelastic scattering of longitudinally polarised leptons off polarised targets in terms of polarised cross sections. The cross sections have been fitted by three different parameterisations in which the isovector and the isoscalar contributions from Regge inspired models have been considered.

We were able to evaluate the Q^2-evolution of the high energy contribution ($W \geq 2$ GeV) to the generalised GDH integral and to provide an accurate estimate for this contribution in the real photon limit. The latter contribution was found to be about one half of the present discrepancy between previous multipole analysis and the GDH sum rule expectations. Therefore a high energy measurement is needed for a precise test of the sum rule. Moreover we also provided a rough estimate of the low energy ($W < 2$ GeV) multi-hadron and non-resonance contribution to the GDH integral.

At present, while waiting for direct and experimental verifications, from the informations coming from unpolarised single-pion photo-production data at low energy and from inclusive polarised electro-production data at high energy, it seems reasonable to conclude that no room is left for a large violation of the GDH sum rule.

References

1. S.B. Gerasimov, Sov. J. Nucl. Phys. **2** (1966) 430; S.D. Drell and A.C. Hearn, Phys. Rev. Lett. **16** (1966) 908.
2. N. Bianchi, Proc. Workshop on Electron Nucleus Scattering, O. Benhar and A. Fabrocini editors, Elba, July 1-5, 1996, p.363 and references therein.
3. I. Karliner, Phys. Rev. **D 7** (1973) 2717. R.L. Workman and R.A. Arndt, Phys. Rev. **D 45** (1992) 1789. A.M. Sandorfi, C.S. Whisnant and M. Khandaker, Phys. Rev. **D 50** (1994) R6681. R.A. Arndt, I.I. Strakovsky and R. Workman, Phys. Rev. **C 53** (1996) 430.
4. D. Drechsel and G.Krein, Phys. Rev. **D 58** (1998) 116009.
5. N.Bianchi and E.Thomas, Phys. Lett. **B 450** (1999) 439.
6. A. Donnachie and P.V. Landshoff, Phys. Lett. **B 296** (1992) 227.
7. R.L. Heimann, Nucl. Phys. **B 64** (1973) 429.
8. Particle Data Group, Phys. Rev. **D 54** (1996) 1.
9. S.D. Bass and P.V. Landshoff, Phys. Lett. **B 336** (1994) 537.
10. EMC Collaboration, J. Ashman *et al.*, Nucl. Phys. **B 328** (1989) 1.
11. SMC Collaboration, B. Adeva *et al.*, Phys. Rev. **D 58** (1998) 112001.
12. E142 Collaboration, P.L. Anthony *et al.*, Phys. Rev. **D 54** (1997) 6620.
13. E143 Collaboration, K. Abe *et al.*, Phys. Rev. **D 58** (1998) 112003.

14. E154 Collaboration, K. Abe *et al.*, Phys. Rev. Lett. **79** (1997) 26.
15. HERMES Collaboration, K. Ackerstaff *et al.*, Phys. Lett. **B 444** (1998) 531; K. Ackerstaff *et al.*, Phys. Lett. **B 404** (1997) 383; A. Airapetian *et al.*, Phys. Lett. **B 442** (1998) 484.
16. A. Levy and U. Maor, Phys. Lett. **B 182** (1986) 108.
17. H. Abramowicz, E.M. Levin, A. Levy and U. Maor, Phys. Lett. **B 269** (1991) 465.
18. A. Capella, A. Kaidalov, C. Merino and J. Tran Thanh Van, Phys. Lett. **B 337** (1994) 358.
19. E155 Collaboration P.L. Anthony *et al.*, hep-ph/9902412
20. S.D. Bass and M.M. Brisudova, Eur. Phys. J. **A 4** (1999) 251.